Geophysical Research Letters

RESEARCH LETTER
10.1029/2025GL115470

Key Points:

- High-frequency data from a mooring in the coastal California current reveals that the region is a net source of CO_2 to the atmosphere
- Monthly average fluxes miss short-term CO_2 flux variability and inaccurately suggest the region is a net CO_2 sink
- High-frequency correlations between winds and pCO_2 induce a net outgassing of CO_2, especially during the spring upwelling season

Supporting Information:

Supporting Information may be found in the online version of this article.

Correspondence to:

R. Song,
ruiming@ucsb.edu

Citation:

Song, R., DeVries, T., Li, R., Sutton, A., Send, U., & Frazão, H. C. (2025). High-frequency correlations between winds and pCO_2 change the California coastal upwelling system from a CO_2 sink to a source. *Geophysical Research Letters*, *52*, e2025GL115470. https://doi.org/10.1029/2025GL115470

Received 27 FEB 2025
Accepted 15 JUN 2025

Author Contributions:

Conceptualization: Tim DeVries
Data curation: Adrienne Sutton, Uwe Send
Formal analysis: Ruiming Song, Renjian Li
Funding acquisition: Tim DeVries
Investigation: Ruiming Song, Tim DeVries
Methodology: Ruiming Song, Tim DeVries
Resources: Adrienne Sutton, Uwe Send
Supervision: Tim DeVries
Visualization: Ruiming Song
Writing – original draft: Ruiming Song

High-Frequency Correlations Between Winds and pCO_2 Change the California Coastal Upwelling System From a CO_2 Sink to a Source

Ruiming Song[1,2], Tim DeVries[1,2], Renjian Li[2], Adrienne Sutton[3], Uwe Send[4], and Helena C. Frazão[4]

[1]Department of Geography, University of California, Santa Barbara, CA, USA, [2]Earth Research Institute, University of California, Santa Barbara, CA, USA, [3]Pacific Marine Environmental Laboratory, National Oceanic and Atmospheric Administration, Seattle, WA, USA, [4]Scripps Institution of Oceanography, University of California San Diego, La Jolla, CA, USA

Abstract Net sea-air CO_2 flux can be calculated from observations of seawater and atmosphere partial pressure of CO_2 (pCO_2) and estimates of the gas transfer velocity. Typically, these quantities are calculated at a monthly resolution, which misses potentially important high-frequency temporal variability. Here, we calculated sea-air CO_2 flux at a 3-hourly resolution using a 10-year mooring data set (2011–2020) from the central California coastal upwelling region. We identified a significant flux of CO_2 from the ocean to the atmosphere due to a positive correlation between seawater pCO_2 and wind speed at timescales of hours to days, particularly during the late spring and early summer upwelling season. Accounting for this variability changes the region from a net sink to a net source of CO_2 to the atmosphere. These findings imply that CO_2 fluxes computed from monthly-resolution data may miss important shorter-term variability that contributes to a net outgassing of CO_2 from the ocean.

Plain Language Summary The exchange of carbon dioxide (CO_2) between the ocean and atmosphere plays a crucial role in regulating Earth's climate. In this study, we examined how accurately this exchange is captured along the California coast, where seasonal wind-driven upwelling brings CO_2-rich waters to the surface. We compared CO_2 flux estimates using data collected every 3 hours for 10 years with those derived from monthly averages. We found that monthly averages often miss important short-term variability, particularly during upwelling seasons. These seasonal changes cause the region to emit more CO_2 into the atmosphere than previously thought, challenging the perception that the coastal California Current is a CO_2 sink. High-frequency calculations revealed that winds and ocean conditions are closely linked, driving this variability in CO_2 exchange. Our findings highlight the need for continuous and high-resolution measurements to better quantify sea-air CO_2 exchange.

1. Introduction

The exchange of carbon dioxide (CO_2) between the ocean and the atmosphere modulates atmospheric CO_2 levels over years to millennia and plays a crucial role in regulating the Earth's climate (DeVries, 2022; Gruber et al., 2023). The global ocean is currently estimated to take up around 2.5 Gt C per year from the atmosphere, representing around 25% of contemporary anthropogenic CO_2 emissions (Friedlingstein et al., 2023; Gruber et al., 2023). However, current estimates of global sea-air CO_2 fluxes have significant uncertainty due to a lack of direct observations and the need to use models to fill in large gaps in the observational record (DeVries et al., 2023; Landschützer et al., 2016; Woolf et al., 2019). Reducing these uncertainties is crucial for understanding the effects of climate change on the ocean carbon sink, and for increasing confidence in future climate projections.

The most common approach for calculating sea-air CO_2 fluxes ($F_{\text{sea-air}}$) uses a bulk formula based on gas transfer velocity (K_w), CO_2 gas solubility (K_0), and the difference between seawater and air partial pressure of CO_2 ($pCO_{2,sw}$ and $pCO_{2,air}$, respectively) (Wanninkhof, 2014)

$$F_{\text{sea-air}} = K_w K_0 \left(pCO_{2,sw} - pCO_{2,air}\right) = K \Delta pCO_2 \quad (1)$$

Writing – review & editing:
Tim DeVries, Renjian Li, Adrienne Sutton, Uwe Send, Helena C. Frazão

The parameters in Equation 1 are generally not measured at global scales, but must be estimated or calculated. The gas transfer velocity is typically parameterized as a function of wind speed or sea state (Deike & Melville, 2018; Lamarre & Melville, 1991; Liss & Merlivat, 1986; Wanninkhof, 1992). These inputs, in turn, are estimated by reanalysis models or satellite data sets, such as CCMP (Mears et al., 2022), ERA (Uppala et al., 2005), JRA (Kobayashi et al., 2015) and WaveWatch3 (Kobayashi et al., 2015; Tolman et al., 2019; Uppala et al., 2005). CO_2 solubility in seawater is derived from seawater salinity and temperature using empirical functions based on laboratory measurements (Weiss, 1974), with salinity and temperature generally estimated by satellite remote sensing or reanalysis products. The seawater pCO_2 is typically estimated by a statistical or machine learning model (e.g., Gregor et al., 2019; Landschützer et al., 2013; Rödenbeck et al., 2022), itself fitted to very sparse observations of seawater pCO_2 from shipboard measurements (e.g., SOCATv2022, Bakker et al., 2022). All of these parameterizations, estimations, and calculations come with uncertainties that propagate through Equation 1, making it challenging to obtain accurate global flux estimates.

One problematic aspect of obtaining accurate estimates of $F_{\text{sea-air}}$ is the large temporal variability of the parameters in Equation 1. The majority of global sea-air CO_2 flux products calculate all of the parameters in Equation 1 at monthly resolution, from which monthly mean estimates of $F_{\text{sea-air}}$ are derived (e.g., Gloege et al., 2022; Landschützer et al., 2016; Wanninkhof et al., 2023). This approach obscures the higher-frequency variability inherent in these parameters (Carroll et al., 2020; Chau et al., 2022; Fiechter et al., 2014) and tends to smooth out short-term fluctuations driven by diurnal cycles, episodic wind events, and transient upwelling episodes, potentially leading to underestimation or overestimation of fluxes during periods of rapid environmental change (Gu et al., 2023). In regions where such high-frequency variability is common, such as those subject to episodic storms or upwelling, using monthly data could therefore lead to biases in calculations of $F_{\text{sea-air}}$.

Several previous studies have examined the influence of short-term variability on sea-air CO_2 fluxes. Sutton et al. (2021) deployed Uncrewed Surface Vehicles in the Southern Ocean to sample hourly resolution data and compared them with data that were temporally averaged over longer periods. They found that subsampling at intervals, such as 10 days, introduced significant biases in CO_2 flux estimates, particularly during periods of high wind variability and storm events. Their findings demonstrated that lower-resolution data can fail to capture the true variability of seawater pCO_2, leading to underestimations or overestimations of CO_2 fluxes. Djeutchouang et al. (2022) used machine learning techniques to reconstruct seawater pCO_2 from high-resolution data collected by various platforms. They found that models trained on high-resolution data performed better than models trained on lower-resolution data, reducing uncertainties and biases in $pCO_{2,sw}$ estimates. Nickford et al. (2024) calculated sea-air CO_2 fluxes with high-resolution in-situ contemporaneous measurements of wind, wave height, and pCO_2 data and compared them with calculations using data from reanalysis products. They showed that using data from reanalysis products led to significant underestimations of CO_2 flux, particularly during periods of high wind speed and storm events. Bates and Merlivat (2001) conducted an analysis using high-frequency (hourly) wind speed and pCO_2 data collected by a drifting buoy near Bermuda. They found that CO_2 fluxes were significantly higher when high-frequency wind data were used, as opposed to daily averages. Friederich et al. (2002) observed high-frequency sea-air CO_2 fluxes during the 1997–1998 El Niño/La Niña event in the California Current. They observed that sea-air CO_2 fluxes were especially strong during relatively brief periods (days to weeks) of enhanced wind speeds, which coincided with upwelling of CO_2-enriched seawater. They suggested that these brief, transient events are likely to have an outsized impact on local CO_2 fluxes (Friederich et al., 2002).

While these previous studies demonstrated a strong influence of small-scale temporal variability on sea-air CO_2 fluxes, they were all based on data gathered over relatively short time periods, with the longest sampling period being two winter seasons over 2 years (Nickford et al., 2024). Here, we address this limitation by employing 10 years of high-resolution (3-hourly) data from the California Current Ecosystem 2 (CCE2) mooring. The CCE2 mooring is located within the eastern boundary of the California Current System, where persistent equatorward winds generate one of the planet's most intense coastal-upwelling regimes and exceptionally high biological productivity (Checkley & Barth, 2009; Huyer, 1983). Quantifying carbon fluxes here is regionally and globally important, as this narrow inner-shelf zone exchanges carbon and nutrients with the larger North Pacific. We use both wind-based and sea-state based parameterizations of gas transfer velocity to calculate sea-air CO_2 fluxes for this decade-long time series. We show that high-frequency (hours to days) temporal correlations between gas transfer velocity and sea-air pCO_2 difference lead to an outgassing of CO_2 at this location, particularly in the late spring and early summer upwelling season. Using monthly data to calculate sea-air CO_2 fluxes at this location

underestimates the efflux of CO_2 from this region, wrongly implying that the region is a net sink rather than a source of CO_2 to the atmosphere. Our findings highlight the necessity of high-temporal-resolution monitoring for accurate sea-air CO_2 flux estimation.

2. Data and Methods

In this study, we used the bulk formula (Equation 1) to calculate sea-air CO_2 fluxes. Throughout this study, we use the following units for the quantities in Equation 1: $F_{\text{sea-air}}$ has units of mol m^{-2} yr^{-1}, ΔpCO_2 has units of µatm, K_0 is the solubility of CO_2 (Weiss, 1974) with units of mol m^{-3} μatm^{-1}, K_w is the gas transfer velocity with units of m yr^{-1}. Therefore, K has units of mol m^{-2} yr^{-1} μatm^{-1}, although for convenience we usually report K with units of mol m^{-2} hr^{-1} atm^{-1}.

2.1. Data and Study Area

Seawater pCO_2 ($pCO_{2,sw}$) and atmospheric pCO_2 ($pCO_{2,air}$) were taken from the CCE2 mooring (position: 34.324°N, 120.814°W) operated by Scripps Institution of Oceanography and carries a $MAPCO_2$ sensor package from NOAA PMEL. The $MAPCO_2$ is an equilibration-based instrument paired with a nondispersive infrared gas analyzer calibrated in situ with reference gas traceable to World Meteorological Organization standards and total measurement uncertainty of <2 µatm for air and seawater pCO_2 (Sutton et al., 2014). The data set also provides sea surface temperature (SST) and sea surface salinity (SSS) from a Sea-Bird Electronics 16plusV2 SeaCAT calibrated annually by the manufacturer with a measurement uncertainty of <0.01°C and 0.05 respectively. All parameters are collected at a 3-hr resolution from 2011 to 2020, with occasional short gaps due to instrument failures (Figure S2 in Supporting Information S1; Sutton et al., 2019).

The study area is located within the inner shelf waters of central and southern California (Figure S1 in Supporting Information S1), a region influenced by seasonal wind-driven coastal upwelling. Temperature and salinity data (Figure S2 in Supporting Information S1) clearly indicate the occurrence of strong upwelling events during the spring season, characterized by minimum SST and maximum SSS values. This seasonal signal aligns closely with the documented timing of peak wind-driven coastal upwelling activity in this region (Huyer, 1983; Jacox et al., 2018). Upwelling events in this region are triggered by intensified equatorward winds (Send et al., 1987; Washburn et al., 2011), which drive carbon-rich waters onto the continental shelf, abruptly increasing surface water $pCO_{2,sw}$ and causing large positive values of ΔpCO_2 (Fassbender et al., 2011; Feely et al., 2008). Upwelling also transports essential nutrients to the surface, fueling phytoplankton blooms which can reduce or reverse the sea-air ΔpCO_2 gradient as they mature (Capone & Hutchins, 2013; Chavez & Messié, 2009; Fassbender et al., 2011; Feely et al., 2008; Leinweber & Gruber, 2013). The combination of these processes can lead to large short-term fluctuations in ΔpCO_2 with uncertain consequences for the net sea-air CO_2 flux (e.g., Chavez et al., 2007; Hales et al., 2005; Takahashi et al., 2009).

2.2. Gas Transfer Velocity Parameterizations

We use two different formulations for the CO_2 gas transfer velocity (K_w) in Equation 1. The first formulation is the widely-used wind-speed based formula of Wanninkhof (1992, 2014). In this formulation, K_w is proportional to the square of the wind speed at 10 m above the sea surface, and the constant of proportionality is computed from estimates of the rate of bomb radiocarbon invasion into the ocean (Wanninkhof, 2014) (hereafter, W14). The second formulation uses a sea-state dependent model for K_w based on wave breaking statistics developed by Deike and Melville (2018), which was simplified to a bulk formula by Reichl and Deike (2020). Here, we use the latest formulation of this model calibrated for CO_2 gas transfer by Zhou et al. (2023). This model expresses K_w as the sum of a component due to bubble entrainment from breaking waves, which is a function of wind speed and wave height, and a component due to molecular diffusion across a turbulent surface without bubbles, which is proportional to the wind friction velocity. See Text S1 in Supporting Information S1 for details of these calculations.

2.3. Climatology and Component Separation

We computed $F_{\text{sea-air}}$ at 3-hourly intervals using Equation 1 for all data available in the records. Then, we developed a monthly climatology by averaging all data within a given month and year, and then averaging across years. A given month and year was admitted into the climatology only if that particular month and year had

greater than 80% data coverage at 3-hourly resolution for both ΔpCO_2 and K. This yielded between 5 and 9 years of data for each month in the climatology, mainly due to gaps in the ΔpCO_2 record (Figure S2 in Supporting Information S1; Figure S3 in Supporting Information S1). See Text S2–S4 in Supporting Information S1 for details.

For this climatology, we also performed a component separation to express the total sea-air flux (Equation 1) as the sum of monthly mean components and deviations from the monthly mean,

$$<F_{\text{sea-air}}> = <K\Delta pCO_2> = <\left(\overline{K} + K'\right) \times \left(\overline{\Delta pCO_2} + \Delta pCO_2'\right)> \quad (2)$$

where the angle brackets indicate a monthly climatology (average of a single month over all years), quantities without bars or primes are the 3-hourly values, the barred quantities are the monthly mean value within each month and year, and the primed quantities are the difference between the 3-hourly values and the monthly mean values (see Text S2 in Supporting Information S1 for details). Expanding Equation 2 yields,

$$<F_{\text{sea-air}}> = <\overline{K} \cdot \overline{\Delta pCO_2}> + <\overline{K} \cdot \Delta pCO_2'> + <K' \cdot \overline{\Delta pCO_2}> + <K' \cdot \Delta pCO_2'> \quad (3)$$

The middle two terms on the right-hand side of Equation 3 should both be 0, since the barred quantities are averages and the primed quantities, by definition, have a mean of 0. In practice, the third term on the right-hand side of Equation 3 may not exactly be zero since K is the product of two quantities, K_w and K_0, which themselves might have some correlation. However, we have found that this term is extremely small.

Thus, simplifying Equation 3 yields to a very close approximation

$$<F_{\text{sea-air}}> = <\overline{K} \cdot \overline{\Delta pCO_2}> + <K' \cdot \Delta pCO_2'>. \quad (4)$$

The first term on the right-hand side of Equation 4 is the sea-air CO_2 flux computed using monthly-averaged values of K and pCO_2, which is the typical temporal resolution of most data-based products. Hereafter, we refer to this term as the "monthly flux." The second term on the right-hand side of Equation 4 is neglected by calculations that use monthly-averaged data. We refer to this term as the "cross-correlation flux," as its magnitude depends on the correlation between the higher-frequency variability of K and ΔpCO_2. If K' and ΔpCO_2' are positively correlated, then the cross-correlation term is positive, while if they are negatively correlated, then the cross-correlation term is negative.

Recently, Gregor et al. (2024) developed a new neural network approach, OceanCarbNN, to compute sea-air CO_2 fluxes at an 8-day, quarter-degree spatial resolution. The 8-day resolution captures more temporal variability compared to traditional monthly products. To investigate the improved accuracy of 8-day resolution calculations compared to monthly resolution calculations, we also performed a component separation using Equation 3 but using 8-day averages instead of monthly averages.

3. Results

3.1. Monthly Climatology of ΔpCO_2 and K

At the CCE2 mooring, the ΔpCO_2 reaches peak values during the spring and early summer from April-June (Figure 1a). This period corresponds to the peak seasonal wind-driven upwelling in the inner shelf waters of central and southern California, which brings high-CO_2 waters from the deep ocean to the surface layer and causes large positive values of ΔpCO_2 (see Section 2.1). The temporal variability of ΔpCO_2 also reaches a peak in the springtime. This variability is likely due to the intermittent upwelling/relaxation cycles in this season (Send et al., 1987; Washburn et al., 2011), combined with the enhanced biological productivity fueled by upwelled nutrients (see Section 2.1). In the summer and fall seasons, upwelling events are less frequent and the mean value of ΔpCO_2 and its variability reach a minimum (Figure 1a).

The gas transfer rate (K) also exhibits seasonal variability, with the highest mean values and variances in the springtime (April-June) (Figure 1b). The overall seasonality of K is driven by seasonal variability in temperature, with lowest temperatures and highest solubilities (K_0) in the springtime, while the variability of K is primarily due to variability in the gas transfer velocity (K_w) driven by variability in wind speeds (Figure S4 in Supporting

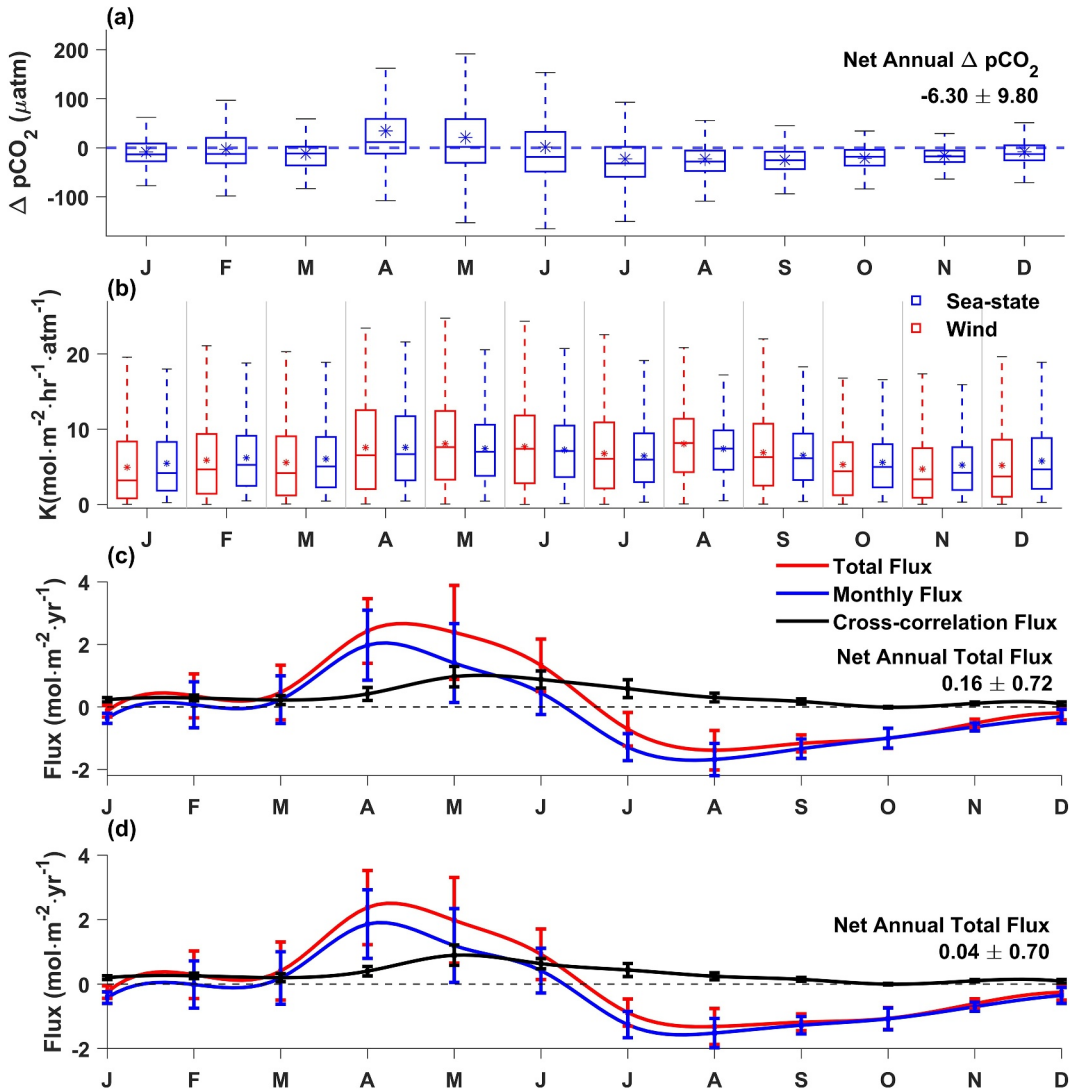

Figure 1. Monthly climatology of (a) the difference between seawater and air pCO_2 ($\Delta pCO_2 = pCO_{2,sw} - pCO_{2,air}$), (b) gas transfer rate K ($K = K_w K_0$) (red for wind-based, blue for sea-state-based), and the sea-air CO_2 flux components computed using the methodology in Section 2.3 using (c) a wind-based gas transfer velocity, and (d) a sea-state-based gas transfer velocity. Stars in (a) and (b) indicate monthly means, and lines mark the 25th, 50th, and 75th percentiles of all 3-hourly data. Whiskers extend to 1.5 times the interquartile range. In panels (c) and (d), the error bars are the standard error of the mean flux for each month, which reflects the interannual variability of each flux component. The curve is a cubic spline interpolation fit through the mean flux for each month.

Information S1). The K values computed by the wind-only parameterization (W14) are slightly larger and more variable than sea-state-based K values (Zhou et al., 2023) during the spring season, and lower and less variable in other months. In this region, K is more sensitive to high wind speeds in W14's approach, because high wind events are often not accompanied by large wave heights in coastal regions. The sea-state-based K values are generally higher than the wind-based K values during the fall and winter seasons (October-March), when wave heights peak along the coastline due to remote storms in the North Pacific (Ma & Zhang, 2018; Méndez et al., 2008).

3.2. Monthly Climatology of Sea-Air CO_2 Fluxes

The monthly climatology of both wind-based and sea-state-based total sea-air CO_2 flux exhibits a seasonal pattern similar to K and ΔpCO_2 (Figures 1c and 1d). The strongest outgassing (positive sea-air CO_2 flux) occurs during the spring upwelling season (April-June). This gives way to negative fluxes (indicating uptake) in the later summer through fall seasons as upwelling weakens and surface waters warm (Walter et al., 2018). High standard

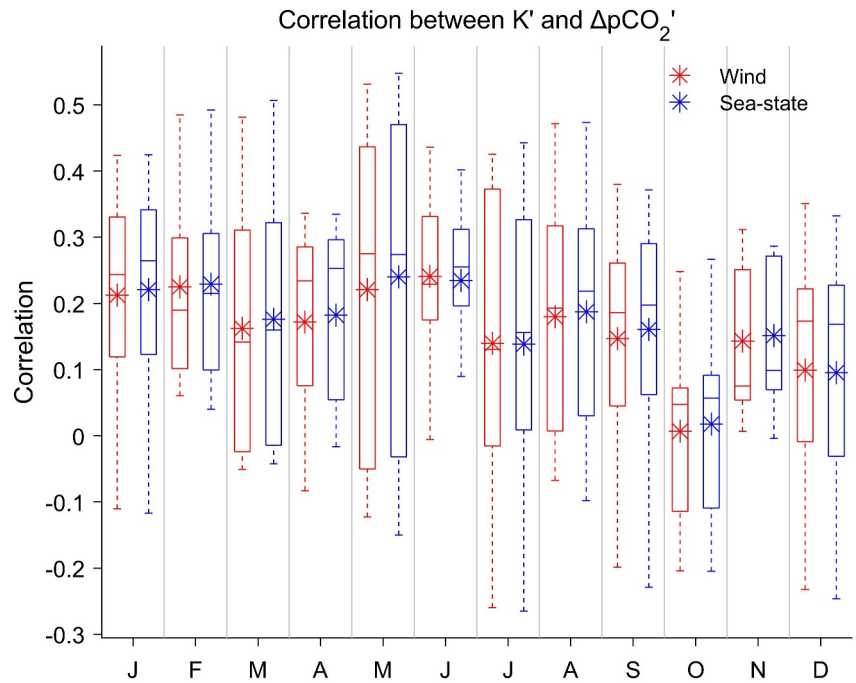

Figure 2. The correlation between high-frequency variations in the gas transfer rate (K') and the sea-air pCO_2 difference ($\Delta pCO_2'$) for each month. Stars indicate monthly means, and lines mark the 25th, 50th, and 75th percentiles of all 3-hourly data for that particular month. Whiskers extend to 1.5 times the interquartile range. Red symbols correspond to gas transfer rates calculated using the wind-based approach (W14), and blue symbols to the sea-state-based approach (Zhou et al., 2023).

errors of the climatology during the upwelling season reflect the high interannual variability of the sea-air CO_2 flux, due to large variability in winds and ΔpCO_2 during this time (cf. Figures 1a and 1b, and Figure S4 in Supporting Information S1).

Notably, the monthly sea-air fluxes calculated using monthly values of K and ΔpCO_2 are always lower than the total flux calculated using 3-hourly data, with the most significant differences occurring from April to August. This difference is due to the cross-correlation flux $K'\Delta pCO_2'$ (Figures 1c and 1d). The cross-correlation flux is consistently positive throughout the year, due to the consistently positive correlation between K' and $\Delta pCO_2'$ (Figure 2). This correlation peaks in the springtime (April-June), coincident with the peak in the variability of ΔpCO_2 (Figures 1a and 1b), which leads to the largest values of the cross-correlation flux during those months (Figures 1c and 1d). The mechanism driving this positive correlation is likely the variability of upwelling events. Strong winds, which correspond to large values of the gas transfer velocity, lead to the upwelling of high-CO_2 waters, which increases ΔpCO_2 and the solubility K_0. These upwelling periods are sporadic and not well captured when using monthly mean values of K and ΔpCO_2.

The wind-based and sea-state based gas transfer parameterizations yield very similar results for both the magnitude and seasonality of the total sea-air CO_2 flux and the cross-correlation flux (Figures 1c and 1d). The largest difference between the two parameterizations occurs in June, when the sea-state approach underestimates the total flux by 0.4 $molm^{-2}\ yr^{-1}$ and the cross-correlation flux by 0.2 $molm^{-2}\ yr^{-1}$ relative to the wind-based method. This consistency across methods underscores the robustness of the observed seasonal patterns.

If the sea-air CO_2 flux is calculated at 8-day rather than monthly resolution (Figure S5 in Supporting Information S1), a similar seasonal pattern to the monthly climatology emerges: outgassing and high variability during spring and early summer, with uptake and weaker variability in later summer through fall and winter. Like in the monthly climatology, the cross-correlation flux is almost always positive, with just a few instances of negative values. However, the magnitude of the cross-correlation flux is reduced by roughly half compared to the monthly climatology, which suggests that small-scale temporal variability is better captured by the 8-day climatology than the monthly climatology.

Table 1
The Annual Mean Sea-Air CO_2 Flux at the CCE2 Mooring and Its Standard Error, in mol m^{-2} yr^{-1}, for Both the Monthly and 8-Day Climatologies, Using Both Wind-Speed Based (W14) and Sea-State Based (Zhou et al., 2023) Gas Transfer Velocity Formulations

Climatology	Gas transfer formulation	Total flux	Monthly flux or 8-day flux	Cross-correlation flux
Monthly	Wind speed	0.16 ± 0.72	−0.21 ± 0.67	0.36 ± 0.18
	Sea state	0.04 ± 0.70	−0.24 ± 0.63	0.30 ± 0.14
8-day	Wind speed	0.12 ± 1.03	−0.06 ± 0.99	0.18 ± 0.20
	Sea state	0.02 ± 0.94	−0.12 ± 0.94	0.16 ± 0.16

Note. The sum of the monthly flux (or 8-day flux) and the cross-correlation flux may not exactly match the total flux due to rounding errors or small values of the third term in Equation 3.

3.3. Annual Mean Sea-Air CO_2 Fluxes

Table 1 summarizes the annual mean of each component of the sea-air CO_2 flux. The annual mean total CO_2 flux is positive (indicating outgassing) for all the methods used here, although there is significant interannual variability as indicated by the large standard error. The annual mean monthly sea-air CO_2 flux is on average negative, indicating net CO_2 uptake by the ocean, although again there is large interannual variability. The annual mean cross-correlation flux is on average positive, with much lower standard error (e.g., lower interannual variability) than the other terms, suggesting that the short-term variability captured by the cross-correlation flux is consistent over time. The annual mean value of the cross-correlation flux is about half as large when using an 8-day climatology compared to the monthly climatology, indicating that roughly half of the cross-correlation flux is due to sub-weekly variability. The sea-state approach has a lower annual mean total flux than that calculated using W14. This is due to slightly stronger uptake when using monthly (or 8-day) fluxes, as well as weaker outgassing due to a smaller value of the cross-correlation flux (Table 1). However, due to the large standard errors, these differences are not statistically significant.

It is surprising that the positive annual mean sea-air CO_2 flux at the CCE2 mooring is juxtaposed with a negative annual mean ΔpCO_2 of −6.3 ± 9.8 μatm (see Figure 1a); similarly, Frazão et al. (2025) report a negative annual mean ΔpCO_2 (−3.4 ± 4.6 μatm) over 2010–2022 at the same location despite a positive annual mean sea-air CO_2 flux. The reason for this is, once again, the positive correlation between ΔpCO_2 and the gas transfer velocity, such that times of high ΔpCO_2 in the springtime are associated with the highest gas transfer velocities.

4. Discussion

The results presented here highlight strong seasonal and short-term variability in the sea-air CO_2 flux in the California Current, driven by large variability in both the gas transfer rate and the ΔpCO_2, and their correlations. Much of this variability appears to be tied to variability in wind speeds, with strong springtime wind events favoring upwelling and outgassing, and weak winds favoring net CO_2 uptake. To further analyze the impact of wind speeds on sea-air CO_2 flux, we calculated the distribution of wind speeds and the corresponding sea-air CO_2 flux (Figure 3). We find two distinct regimes. The low wind speed regime corresponds to wind speeds of less than 11 m/s, during which there is net CO_2 uptake and the magnitude of the cross-correlation term is small. This low wind speed regime accounts for 75.5% of the observations. In the high wind speed regime (>11 m/s), there is a net CO_2 outgassing, with stronger wind speeds leading to a sharp increase in the net sea-air CO_2 flux. Although the high wind speed regime accounts for only 24.5% of the observations, it accounts for the net annual outgassing in this region. Notably, the cross-correlation flux accounts for roughly 30%–40% of the net outgassing in this high wind speed regime. Without accounting for the cross-correlation flux, the sea-air CO_2 flux at higher wind speeds will be significantly underestimated. This analysis confirms the suggestions of Friederich et al. (2002) based on their findings from the 1997–1998 El Niño/La Niña event—that is, transient high-wind-speed events have an outsized influence on sea-air CO_2 fluxes in this region, and much of this influence is due to correlations between wind speeds and seawater pCO_2.

An important implication of these findings is that, because of the sensitive dependence of the CO_2 flux (and particularly the cross-correlation flux) on wind speed, it is important to use accurate high-resolution winds that capture local conditions. Sharp et al. (2022) calculated the sea-air CO_2 flux in 2015 using the same 3-hourly

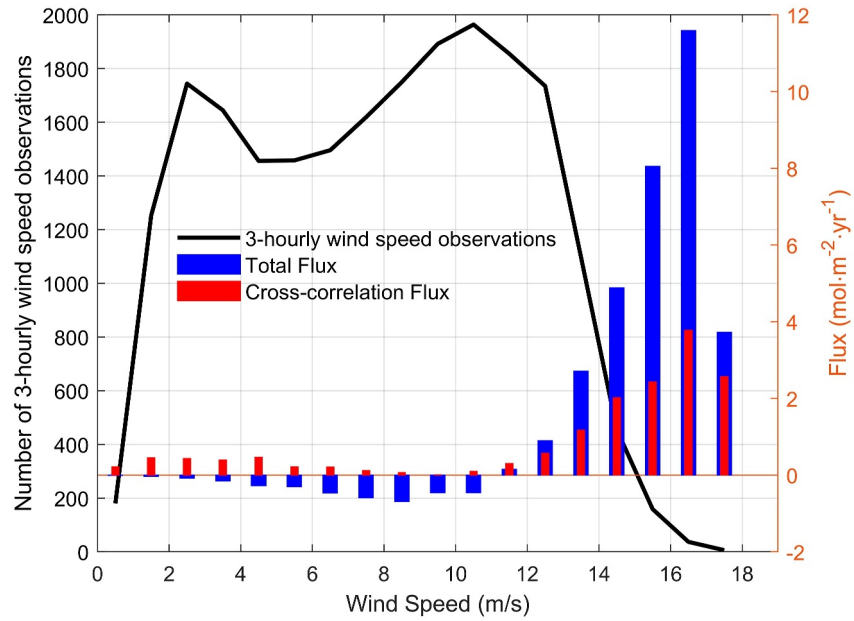

Figure 3. Wind distribution and average sea-air CO_2 flux calculated using the W14 parameterization for K_w. The black curve shows the number of wind speed observations, discretized at 1 m/s intervals. The histogram shows the corresponding net sea-air CO_2 flux at each wind speed interval. The blue bars are the net sea-air CO_2 flux computed from 3-hourly resolution data, and the red bars represent the value of the cross-correlation flux.

resolution CCE2 data used here, and obtained an annual mean sea-air CO_2 flux of −0.18 mol m^{-2} yr^{-1} using the W14 formulation. However, we calculated an annual mean sea-air CO_2 flux in 2015 of −0.43 mol m^{-2} yr^{-1} using the W14 formulation (−0.45 mol m^{-2} yr^{-1} using the sea-state formulation; Figure S6 in Supporting Information S1). The key difference between our methods lies in the choice of wind speed data: we utilized in-situ wind measurements from the nearby West Santa Barbara buoy, while Sharp et al. (2022) used winds from the ERA5 reanalysis product. The meteorological buoy data should capture localized wind conditions specific to the region better than the reanalysis product, including higher wind speeds during upwelling events, which can be underrepresented in reanalysis products (Nickford et al., 2024). This aligns with findings from Nickford et al. (2024), who found that substituting in-situ wind measurements with reanalysis winds underestimated CO_2 uptake by up to 9%, particularly during high wind conditions.

5. Conclusions

Our study provides a detailed analysis of the seasonal and short-term variability in sea-air CO_2 fluxes in the nearshore California Current. By developing a climatology of sea-air CO_2 fluxes from 10 years of 3-hourly resolution data, we found that the net sea-air CO_2 flux along the outer California shelf is strongly positive (outgassing) in the springtime upwelling season, and weakly negative during most other seasons. On average, this leads to a net annual outgassing of CO_2 at this location of 0.16 ± 0.72 mol m^{-2} yr^{-1} using the W14 gas transfer formulation, as opposed to a negative flux (uptake) of −0.21 mol m^{-2} yr^{-1} (−0.06 mol m^{-2} yr^{-1}) if only monthly (8-day) data are used. It should be noted that this seasonal pattern is superimposed on significant year-to-year variability in the sea-air CO_2 fluxes, rendering the long-term mean flux reported here only appropriate for the 2011–2020 period.

A significant driver of the overall net outgassing of CO_2 at this location is the correlation between high-frequency gas transfer rates and seawater pCO_2. Here, we defined a "cross-correlation flux" to explain the difference between the sea-air CO_2 flux computed from high-resolution (3-hourly) data and that computed from monthly data. The magnitude of this cross-correlation flux was 0.36 ± 0.18 mol m^{-2} yr^{-1} when using the W14 gas transfer formulation. For comparison, the net sea-air CO_2 flux for the global coastal ocean is −0.48 mol m^{-2} yr^{-1}, based on a compilation of monthly-averaged pCO_2 products (Resplandy et al., 2024). Thus, if the magnitude of the cross-correlation term in other coastal regions is similar to that in the coastal California current, this commonly

neglected term could dramatically weaken the CO_2 sink of coastal ocean. This illustrates the critical need to assess the cross-correlation fluxes in other coastal regions, since high-frequency variability in pCO_2 and wind has been commonly observed (e.g., Gago et al., 2003; Li et al., 2020; Saderne et al., 2013).

Several other key findings emerge from our study. First, the influence of higher-frequency variability on the net sea-air CO_2 flux depends on the gas transfer parameterization used. Overall, we found a slightly higher influence when using a wind-based parameterization (W14) than a sea-state based parameterization (Zhou et al., 2023). Second, because the sea-air CO_2 flux (and especially the magnitude of the cross-correlation flux) is very sensitive to the wind speed distribution and the frequency of high-wind events, it is important to compute sea-air CO_2 fluxes using an accurate wind product. Here, we used local winds from a nearby meteorological buoy, which have been shown to better capture high-wind conditions than reanalysis wind products (e.g., Chiodi et al., 2019; Nickford et al., 2024). Overall, our findings emphasize the need for continuous and high-frequency measurements to accurately capture the complex dynamics of sea-air CO_2 fluxes, particularly in coastal upwelling regions. It remains an open question whether high-frequency variability plays a large role in determining the magnitude of the global ocean carbon sink, but based on the results presented here, it would be prudent to investigate this.

Conflict of Interest

The authors declare no conflicts of interest relevant to this study.

Data Availability Statement

The pCO_2 time series mooring data used in this study are supported by the Office of Oceanic and Atmospheric Research of NOAA, U.S. Department of Commerce (accessible at https://doi.org/10.3334/cdiac/otg.tsm_cce2_121w_34n), as described in Sutton et al. (2012). The wind data are from the National Data Buoy Center (2025) at station 46054 (available at https://www.ndbc.noaa.gov/station_history.php?station=46054). All data, codes and figures are on Zenodo at Song (2025) https://doi.org/10.5281/zenodo.14590992.

Acknowledgments

TD acknowledges support from NSF Grant OCE-1948955. We acknowledge the Office of Oceanic and Atmospheric Research of NOAA, U.S. Department of Commerce, including resources from the Global Ocean Monitoring and Observing Program and the Ocean Acidification Program: Open Funder Registry numbers 100018302 and 100018228, respectively. The CCE2 mooring is supported by NOAA Grant NA20OAR4320278, and is part of the global OceanSITES program. We also acknowledge the National Data Buoy Center for making the wind speed data from station 46054. This is PMEL contribution 5731.

References

Bakker, D. C. E., Alin, S. R., Becker, M., Bittig, H. C., Castaño-Primo, R., Feely, R. A., et al. (2022). Surface ocean CO_2 atlas database version 2022 (SOCATv2022) (ncei accession 0253659). https://doi.org/10.25921/1H9F-NB73

Bates, N. R., & Merlivat, L. (2001). The influence of short-term wind variability on air–sea CO_2 exchange. *Geophysical Research Letters*, *28*(17), 3281–3284. https://doi.org/10.1029/2001GL012897

Capone, D. G., & Hutchins, D. A. (2013). Microbial biogeochemistry of coastal upwelling regimes in a changing ocean. *Nature Geoscience*, *6*(9), 711–717. https://doi.org/10.1038/ngeo1916

Carroll, D., Menemenlis, D., Adkins, J. F., Bowman, K. W., Brix, H., Dutkiewicz, S., et al. (2020). The ECCO-Darwin data-assimilative global ocean biogeochemistry model: Estimates of seasonal to multidecadal surface ocean pCO_2 and air-sea CO_2 flux. *Journal of Advances in Modeling Earth Systems*, *12*(10), e2019MS001888. https://doi.org/10.1029/2019MS001888

Chau, T. T. T., Gehlen, M., & Chevallier, F. (2022). A seamless ensemble-based reconstruction of surface ocean pCO_2 and air–sea CO_2 fluxes over the global coastal and open oceans. *Biogeosciences*, *19*(4), 1087–1109. https://doi.org/10.5194/bg-19-1087-2022

Chavez, F. P., & Messié, M. (2009). A comparison of eastern boundary upwelling ecosystems. *Progress in Oceanography*, *83*(1–4), 80–96. https://doi.org/10.1016/j.pocean.2009.07.032

Chavez, F. P., Takahashi, T., Cai, W.-J., Friederich, G., Hales, B., Wanninkhof, R., & Feely, R. (2007). Coastal oceans. The first state of the carbon cycle report (SOCCR): The North American carbon budget and implications for the global carbon cycle (pp. 157–166). Retrieved from https://www.researchgate.net/publication/291939644_Coastal_oceans

Checkley Jr., D. M., & Barth, J. A. (2009). Patterns and processes in the California current system. *Progress in Oceanography*, *83*(1–4), 49–64. https://doi.org/10.1016/j.pocean.2009.07.028

Chiodi, A. M., Dunne, J. P., & Harrison, D. E. (2019). Estimating air-sea carbon flux uncertainty over the tropical Pacific: Importance of winds and wind analysis uncertainty. *Global Biogeochemical Cycles*, *33*(3), 370–390. https://doi.org/10.1029/2018GB006047

Deike, L., & Melville, W. K. (2018). Gas transfer by breaking waves. *Geophysical Research Letters*, *45*(19), 10482–10492. https://doi.org/10.1029/2018GL078633

DeVries, T. (2022). The ocean carbon cycle. *Annual Review of Environment and Resources*, *47*(1), 317–341. https://doi.org/10.1146/annurev-environ-120920-111307

DeVries, T., Yamamoto, K., Wanninkhof, R., Gruber, N., Hauck, J., Müller, J. D., et al. (2023). Magnitude, trends, and variability of the global ocean carbon sink from 1985 to 2018. *Global Biogeochemical Cycles*, *37*(10), e2023GB007780. https://doi.org/10.1029/2023GB007780

Djeutchouang, L. M., Chang, N., Gregor, L., Vichi, M., & Monteiro, P. M. (2022). The sensitivity of pCO_2 reconstructions to sampling scales across a Southern Ocean sub-domain: A semi-idealized ocean sampling simulation approach. *Biogeosciences*, *19*(17), 4171–4195. https://doi.org/10.5194/bg-19-4171-2022

Fassbender, A. J., Sabine, C. L., Feely, R. A., Langdon, C., & Mordy, C. W. (2011). Inorganic carbon dynamics during northern California coastal upwelling. *Continental Shelf Research*, *31*(11), 1180–1192. https://doi.org/10.1016/j.csr.2011.04.006

Feely, R. A., Sabine, C. L., Hernandez-Ayon, J. M., Ianson, D., & Hales, B. (2008). Evidence for upwelling of corrosive "acidified" water onto the continental shelf. *Science*, *320*(5882), 1490–1492. https://doi.org/10.1126/science.1155676

Fiechter, J., Curchitser, E. N., Edwards, C. A., Chai, F., Goebel, N. L., & Chavez, F. P. (2014). Air-sea CO_2 fluxes in the California current: Impacts of model resolution and coastal topography. *Global Biogeochemical Cycles*, *28*(4), 371–385. https://doi.org/10.1002/2013GB004683

Frazão, H. C., Send, U., Sutton, A. J., Ohman, M. D., Lankhorst, M., Martz, T. R., & Sevadjian, J. (2025). Open ocean versus upwelling regimes: Air-sea CO_2 fluxes and pCO_2 inter-annual variability in the Southern California Current System. *Journal of Geophysical Research: Oceans*, *130*, e2024JC022126. https://doi.org/10.1029/2024JC022126

Friederich, G. E., Walz, P. M., Burczynski, M. G., & Chavez, F. P. (2002). Inorganic carbon in the central California upwelling system during the 1997–1999 El Niño–La Niña event. *Progress in Oceanography*, *54*(1–4), 185–203. https://doi.org/10.1016/S0079-6611(02)00049-6

Friedlingstein, P., O'sullivan, M., Jones, M. W., Andrew, R. M., Bakker, D. C., Hauck, J., et al. (2023). Global carbon budget 2023. *Earth System Science Data*, *15*(12), 5301–5369. https://doi.org/10.5194/essd-15-5301-2023

Gago, J., Gilcoto, M., Pérez, F. F., & Rıos, A. (2003). Short-term variability of fCO2 in seawater and air–sea CO_2 fluxes in a coastal upwelling system (Rıa de Vigo, NW Spain). *Marine Chemistry*, *80*(4), 247–264. https://doi.org/10.1016/S0304-4203(02)00117-2

Gloege, L., Yan, M., Zheng, T., & McKinley, G. A. (2022). Improved quantification of ocean carbon uptake by using machine learning to merge global models and pCO_2 data. *Journal of Advances in Modeling Earth Systems*, *14*(2), e2021MS002620. https://doi.org/10.1029/2021MS002620

Gregor, L., Lebehot, A. D., Kok, S., & Scheel Monteiro, P. M. (2019). A comparative assessment of the uncertainties of global surface ocean CO_2 estimates using a machine-learning ensemble (CSIR-ML6 version 2019a)–Have we hit the wall? *Geoscientific Model Development*, *12*(12), 5113–5136. https://doi.org/10.5194/gmd-12-5113-2019

Gregor, L., Shutler, J., & Gruber, N. (2024). High-resolution variability of the ocean carbon sink. *Global Biogeochemical Cycles*, *38*(8), e2024GB008127. https://doi.org/10.1029/2024GB008127

Gruber, N., Bakker, D. C., DeVries, T., Gregor, L., Hauck, J., Landschützer, P., et al. (2023). Trends and variability in the ocean carbon sink. *Nature Reviews Earth & Environment*, *4*(2), 119–134. https://doi.org/10.1038/s43017-022-00381-x

Gu, Y., Katul, G. G., & Cassar, N. (2023). Multiscale temporal variability of the global air-sea CO_2 flux anomaly. *Journal of Geophysical Research: Biogeosciences*, *128*(6), e2022JG006934. https://doi.org/10.1029/2022JG006934

Hales, B., Takahashi, T., & Bandstra, L. (2005). Atmospheric CO_2 uptake by a coastal upwelling system. *Global Biogeochemical Cycles*, *19*(1), GB1009. https://doi.org/10.1029/2004GB002295

Huyer, A. (1983). Coastal upwelling in the California Current system. *Progress in Oceanography*, *12*(3), 259–284. https://doi.org/10.1016/0079-6611(83)90010-1

Jacox, M. G., Edwards, C. A., Hazen, E. L., & Bograd, S. J. (2018). Coastal upwelling revisited: Ekman, Bakun, and improved upwelling indices for the US West Coast. *Journal of Geophysical Research: Oceans*, *123*(10), 7332–7350. https://doi.org/10.1029/2018JC014187

Kobayashi, S., Ota, Y., Harada, Y., Ebita, A., Moriya, M., Onoda, H., et al. (2015). The JRA-55 reanalysis: General specifications and basic characteristics. *Journal of the Meteorological Society of Japanese Series II*, *93*(1), 5–48. https://doi.org/10.2151/jmsj.2015-001

Lamarre, E., & Melville, W. K. (1991). Air entrainment and dissipation in breaking waves. *Nature*, *351*(6326), 469–472. https://doi.org/10.1038/351469a0

Landschützer, P., Gruber, N., & Bakker, D. C. (2016). Decadal variations and trends of the global ocean carbon sink. *Global Biogeochemical Cycles*, *30*(10), 1396–1417. https://doi.org/10.1002/2015GB005359

Landschützer, P., Gruber, N., Bakker, D. C., Schuster, U., Nakaoka, S. I., Payne, M. R., et al. (2013). A neural network-based estimate of the seasonal to inter-annual variability of the Atlantic Ocean carbon sink. *Biogeosciences*, *10*(11), 7793–7815. https://doi.org/10.5194/bg-10-7793-2013

Leinweber, A., & Gruber, N. (2013). Variability and trends of Ocean Acidification in the southern California current system: A time series from Santa Monica Bay. *Journal of Geophysical Research: Oceans*, *118*(7), 3622–3633. https://doi.org/10.1002/jgrc.20259

Li, M., Li, R., Cai, W. J., Testa, J. M., & Shen, C. (2020). Effects of wind-driven lateral upwelling on estuarine carbonate chemistry. *Frontiers in Marine Science*, *7*, 588465. https://doi.org/10.3389/fmars.2020.588465

Liss, P. S., & Merlivat, L. (1986). Air–sea gas exchange rates: Introduction and synthesis. In P. Buat-Ménard (Ed.), *The role of air–sea exchange in geochemical cycling* (pp. 113–127). Springer. https://doi.org/10.1007/978-94-009-4738-2_5

Ma, X., & Zhang, Y. (2018). Interannual variability of the North Pacific winter storm track and its relationship with extratropical atmospheric circulation. *Climate Dynamics*, *51*(9–10), 3685–3698. https://doi.org/10.1007/s00382-018-4104-8

Mears, C., Lee, T., Ricciardulli, L., Wang, X., & Wentz, F. (2022). Improving the accuracy of the Cross-Calibrated Multi-Platform (CCMP) ocean vector winds. *Remote Sensing*, *14*(17), 4230. https://doi.org/10.3390/rs14174230

Méndez, F. J., Menéndez, M., Luceño, A., Medina, R., & Graham, N. E. (2008). Seasonality and duration in extreme value distributions of significant wave height. *Ocean Engineering*, *35*(1), 131–138. https://doi.org/10.1016/j.oceaneng.2007.07.012

National Data Buoy Center. (2025). Wind data from station 46054 [Dataset]. *NOAA National Data Buoy Center. Public domain*. Retrieved from https://www.ndbc.noaa.gov/station_history.php?station=46054

Nickford, S., Palter, J. B., & Mu, L. (2024). The importance of contemporaneous wind and pCO_2 measurements for regional air–sea CO_2 flux estimates. *Journal of Geophysical Research: Oceans*, *129*(6), e2023JC020744. https://doi.org/10.1029/2023JC020744

Reichl, B. G., & Deike, L. (2020). Contribution of sea-state dependent bubbles to air-sea carbon dioxide fluxes. *Geophysical Research Letters*, *47*(9), e2020GL087267. https://doi.org/10.1029/2020GL087267

Resplandy, L., Hogikyan, A., Müller, J. D., Najjar, R. G., Bange, H. W., Bianchi, D., et al. (2024). A synthesis of global coastal ocean greenhouse gas fluxes. *Global Biogeochemical Cycles*, *38*(1), e2023GB007803. https://doi.org/10.1029/2023GB007803

Rödenbeck, C., DeVries, T., Hauck, J., Le Quéré, C., & Keeling, R. F. (2022). Data-based estimates of interannual sea–air CO_2 flux variations 1957–2020 and their relation to environmental drivers. *Biogeosciences*, *19*(7), 2627–2656. https://doi.org/10.5194/bg-19-2627-2022

Saderne, V., Fietzek, P., & Herman, P. M. J. (2013). Extreme variations of pCO2 and pH in a macrophyte meadow of the Baltic sea in summer: Evidence of the effect of photosynthesis and local upwelling. *PLoS One*, *8*(4), e62689. https://doi.org/10.1371/journal.pone.0062689

Send, U., Beardsley, R. C., & Winant, C. D. (1987). Relaxation from upwelling in the coastal ocean dynamics experiment. *Journal of Geophysical Research*, *92*(C2), 1683–1698. https://doi.org/10.1029/JC092iC02p01683

Sharp, J. D., Fassbender, A. J., Carter, B. R., Lavin, P. D., & Sutton, A. J. (2022). A monthly surface pCO_2 product for the California Current Large Marine Ecosystem. *Earth System Science Data*, *14*(4), 2081–2108. https://doi.org/10.5194/essd-14-2081-2022

Song, R. (2025). Code and figure-generation scripts for "High-resolution estimates of air–sea CO_2 flux in the coastal California Current" (Version 1.0) [Dataset]. *Zenodo. CC-BY 4.0*. https://doi.org/10.5281/zenodo.14590992

Sutton, A. J., Feely, R. A., Maenner-Jones, S., Musielwicz, S., Osborne, J., Dietrich, C., et al. (2019). Autonomous seawater pCO_2 and pH time series from 40 surface buoys and the emergence of anthropogenic trends. *Earth System Science Data*, *11*(1), 421–439. https://doi.org/10.5194/essd-11-421-2019

Sutton, A. J., Sabine, C. L., Maenner-Jones, S., Lawrence-Slavas, N., Meinig, C., Feely, R. A., et al. (2014). A high-frequency atmospheric and seawater pCO2 data set from 14 open-ocean sites using a moored autonomous system. *Earth System Science Data*, *6*(2), 353–366. https://doi.org/10.5194/essd-6-353-2014

Sutton, A. J., Sabine, C. L., Send, U., Ohman, M. D., Musielewicz, S., Maenner Jones, S., et al. (2012). High-resolution ocean and atmosphere pCO_2 time-series measurements from mooring CCE2_121W_34N in the North Pacific ocean (NCEI accession 0084099) [Dataset]. *NOAA National Centers for Environmental Information*. https://doi.org/10.3334/cdiac/otg.tsm_cce2_121w_34n

Sutton, A. J., Williams, N. L., & Tilbrook, B. (2021). Constraining Southern Ocean CO_2 flux uncertainty using uncrewed surface vehicle observations. *Geophysical Research Letters*, *48*(3), e2020GL091748. https://doi.org/10.1029/2020GL091748

Takahashi, T., Sutherland, S. C., Wanninkhof, R., Sweeney, C., Feely, R. A., Chipman, D. W., et al. (2009). Climatological mean and decadal change in surface ocean pCO_2, and net sea–air CO_2 flux over the global oceans. *Deep Sea Research Part II: Topical Studies in Oceanography*, *56*(8–10), 554–577. https://doi.org/10.1016/j.dsr2.2008.12.009

Tolman, H., Abdolali, A., Accensi, M., Alves, J.-H., Ardhuin, F., Babanin, A., et al. (2019). User manual and system documentation of WAVEWATCH III® version 6.07. [Technical report].

Uppala, S. M., Kållberg, P. W., Simmons, A. J., Andrae, U., Bechtold, V. D. C., Fiorino, M., et al. (2005). The ERA-40 re-analysis. *Quarterly Journal of the Royal Meteorological Society*, *131*(612), 2961–3012. https://doi.org/10.1256/qj.04.176

Walter, R. K., Armenta, K. J., Shearer, B., Robbins, I., & Steinbeck, J. (2018). Coastal upwelling seasonality and variability of temperature and chlorophyll in a small coastal embayment. *Continental Shelf Research*, *154*, 9–18. https://doi.org/10.1016/j.csr.2018.01.002

Wanninkhof, R. (1992). Relationship between wind speed and gas exchange over the ocean. *Journal of Geophysical Research*, *97*(C5), 7373–7382. https://doi.org/10.1029/92JC00188

Wanninkhof, R. (2014). Relationship between wind speed and gas exchange over the ocean revisited. *Limnology and Oceanography: Methods*, *12*(6), 351–362. https://doi.org/10.4319/lom.2014.12.351

Wanninkhof, R., Triñanes, J., Pierrot, D., Munro, D. R., Sweeney, C., & Fay, A. R. (2023). Impact of predictor variables on estimates of global sea–air CO_2 fluxes using an Extra Trees machine learning approach. *Authorea Preprints*. https://doi.org/10.22541/essoar.169945403.39061946/v1

Washburn, L., Fewings, M. R., Melton, C., & Gotschalk, C. (2011). The propagating response of coastal circulation due to wind relaxations along the central California coast. *Journal of Geophysical Research*, *116*(C12), C12028. https://doi.org/10.1029/2011JC007502

Weiss, R. (1974). Carbon dioxide in water and seawater: The solubility of a non-ideal gas. *Marine Chemistry*, *2*(3), 203–215. https://doi.org/10.1016/0304-4203(74)90015-2

Woolf, D. K., Shutler, J. D., Goddijn-Murphy, L., Watson, A. J., Chapron, B., Nightingale, P. D., et al. (2019). Key uncertainties in the recent air–sea flux of CO_2. *Global Biogeochemical Cycles*, *33*(12), 1548–1563. https://doi.org/10.1029/2018GB006041

Zhou, X., Reichl, B. G., Romero, L., & Deike, L. (2023). A sea state dependent gas transfer velocity for CO_2 unifying theory, model, and field data. *Earth and Space Science*, *10*(11), e2023EA003237. https://doi.org/10.1029/2023EA003237

References From the Supporting Information

Edson, J. B., Jampana, V., Weller, R. A., Bigorre, S. P., Plueddemann, A. J., Fairall, C. W., et al. (2013). On the exchange of momentum over the open ocean. *Journal of Physical Oceanography*, *43*(8), 1589–1610. https://doi.org/10.1175/JPO-D-12-0173.1

Sutton, A. J., Wanninkhof, R., Sabine, C. L., Feely, R. A., Cronin, M. F., & Weller, R. A. (2017). Variability and trends in surface seawater pCO_2 and CO_2 flux in the Pacific Ocean. *Geophysical Research Letters*, *44*(11), 5627–5636. https://doi.org/10.1002/2017GL073814